HEFAT2010
7th International Conference on Heat Transfer, Fluid Mechanics and Thermodynamics
19-21 July 2010
Antalya, Turkey

UNSTEADY FLOW AROUND TWO SQUARE CYLINDERS IN STAGGERED ARRANGEMENTS

Mahir N*, Altaç Z, Ünver E, Pargan A R, Gelgeç M and Çebi F
*Author for correspondence
Department of Mechanical Engineering,
Eskişehir Osmangazi University,
School of Engineering and Architecture
Eskişehir 27480, TURKEY
E-mail: nmahir@ogu.edu.tr

ABSTRACT

In this study, the flow around two staggered square cylinders, placed in a uniform flow field, has been studied. The numerical simulations have been performed by use of a commercial CFD software Fluent. The Reynolds number, defined as a function of cylinder width D, has been chosen as 100 and 200. In the simulations, the dimensionless distance P/D, between the cylinder centers was changed from 2 to 5, and the incidence angle θ also has been changed from 0^o to 90^o by 25^o increments. In order to evaluate the flow field, isovorticity curves were obtained at different values of dimensionless distance P/D and incidence angle θ. The deviation of the mean drag coefficients and of the square root values of the lift coefficient with P/D and θ also determined. The power spectrums of the lift coefficient have been obtained for different flow fields.

INTRODUCTION

Various two cylinder arrangements have been widely used in many engineering applications such as heat exchangers, cooling of electrical equipments, structures exposed to winds or waves, etc. In these configurations, not only the distance between the cylinders but also their position with respect to other cylinders plays an important role in determining the interference between them.

Most of the experimental and numerical studies about the various arrangements of the cylinders have been performed on the circular cylinders. Existing studies on square cylinders are limited, and most of these studies are based on either tandem or side-by side arrangements of the cylinders.

The interference between the cylinder will start when the downstream cylinder in the wake of upstream one or outside of the wake but sufficiently close two upstream one. Zdravkovich [1] categorized the cylinder interactions as proximity interference and wake interference by considering the location of the second cylinder in or outside of the wake of first one. When the cylinders are close, both vortex streets formed behind cylinder are affected by the interference. The only downstream cylinder is affected for sufficiently large spacing between them.

NOMENCLATURE

C_D	[-]	Drag coefficient
C_L	[-]	Lift coefficient
D	[m]	Side length of cylinders
F	[N]	Force
P	[m]	Axial distance between two cylinders
p	[N/m^2]	Pressure
Re	$U_\infty D/\nu$	Reynolds number
u,v	[m/s]	Velocity components
U_∞	[m/s]	Free stream velocity
x, y	[m]	Cartesian coordinate system

Special characters

ρ	[kg/m^3]	Density
θ	[deg]	Incidence angle
υ	[m/s^2]	Kinematic viscosity

Subscripts

x,y	Direction

Sumner et al. [2] classified flow patterns between and the downstream of the cylinders for centre-to-centre pitch ratio 1 to 5 and angle of the incidence 0^o to 90^o. Their study also reveals that vortex shedding frequencies are associated with individual shear layers rather than individual cylinders, and the vorticies formed from the two separated shear layers of downstream cylinder shed at different frequencies.

Aerodynamic force and vortex shedding frequency measurements for two staggered circular cylinders have been performed by Sumner et al. [3] at the pitch ratios of 1.125 to 4 and for the incidence angles of 0^o to 90^o. From the behavior of the experimental data, they classified the configuration of the cylinders as closely spaced ($P/D < 1.5$), moderate spaced ($1.5 \leq P/D \leq 2.5$) and widely spaced ($P/D > 2.5$). Characteristics of the closely spaced cylinders were the same measured frequency

behind both cylinders and the large changes at the magnitude of the mean aerodynamic forces. At the moderate spaced cylinders, two Strouhal numbers are measured for most incidence angles and for small changes in the mean aerodynamic forces, but relatively complex behavior of the mean aerodynamic forces on the downstream cylinder were observed. Widely spaced cylinders are characterized by single Strouhal number for both cylinders at all incidence angles, and similar mean aerodynamic forces on the upstream cylinder that of on the single cylinder.

Price and Paidoussis [4] also measured drag and lift forces on the group of two and three circular cylinders. They clarified the downstream cylinder locations in the staggered arrangement so that the acting drag and the lift forces on the upstream cylinder are maximum or minimum. On the basis of pressure measurement and flow visiualization, Gu and Sun [5] observed two different pressure patterns, which creates discontinuity of large lift forces on the cylinders, at critical angles. A numerical study of tandem and staggered cylinders has been performed by Mittai et al. [6] for Reynolds numbers of 100 and 1000. They observed very large unsteady forces on the down stream cylinder, which is in the wake of upstream one. Carmo et al. [7] studied wake transition of the flow around two circular cylinders in staggered arrangements. Their 3-D simulations reveal the existence of the C mode instability in addition to A and B type instabilities observed in the spanwise direction of single cylinder wake. Another numerical simulation performed by Jester and Kallinderis [8] for tandem, staggered and side-by-side arrangement of two circular cylinders at Reynolds numbers of 80 and 1000. They have reproduce experimentally observed flow physics such as hysteresis effects and bistable biased flow in tandem cylinders.

Foregoing experimental studies are on the staggered arrangement of the cylinders performed at circular cylinders and higher Reynolds numbers. Limited number of the numerical study exists at laminar flows and circular cylinders. In this study, staggered arrangement of the two square cylinders is considered. The flow patterns around the cylinders and corresponding unsteady forces on the cylinders are investigated at different P/D ratios and incidence angles. Some of the flow patterns, which exist at the wake of circular cylinders in staggered arrangement and high Reynolds numbers, reproduced.

MATHEMATICAL MODEL AND NUMERICAL METHOD

The governing equations, for unsteady incompressible viscous flow, are, for continuity

$$\frac{\partial u}{\partial x}+\frac{\partial v}{\partial y}=0 \qquad (1)$$

for the momentum

$$\frac{\partial u}{\partial t}+u\frac{\partial u}{\partial x}+v\frac{\partial u}{\partial y}=-\frac{1}{\rho}\frac{\partial p}{\partial x}+\upsilon\left(\frac{\partial^2 u}{\partial x^2}+\frac{\partial^2 u}{\partial y^2}\right)$$
$$\frac{\partial v}{\partial t}+u\frac{\partial v}{\partial x}+v\frac{\partial v}{\partial y}=-\frac{1}{\rho}\frac{\partial p}{\partial y}+\upsilon\left(\frac{\partial^2 v}{\partial x^2}+\frac{\partial^2 v}{\partial y^2}\right) \qquad (2)$$

where u and v are the velocity components, p is the pressure, υ is the kinematic viscosity, ρ is the density of the fluid.

The foregoing flow equations are subject to the following boundary conditions:

For the inlet : $u = U_\infty$

For the outlet : $\partial u/\partial x = \partial v/\partial x = 0$

For the bottom and top boundaries: $u = U_\infty, v = 0$ (3)

For the cylinder walls: $u = v = 0$

where U_∞ is the free stream velocity. The lift and drag coefficients are calculated from

$$C_L = 2F_y/\rho D U_\infty^2, \quad C_D = 2F_x/\rho D U_\infty^2 \qquad (4)$$

The flow simulation around two square cylinder in cross flow is numerically performed using the wel-known CFD code FLUENT® [9]. FLUENT code verification in such cross flow problems were performed by Mahir and Altac [10]. Triangular elements and non-uniform grid structure were used for the computational domain. A condensed grid structure has been applied between the cylinders and to the cylinder walls since the interactions between the boundary layer separation from cylinders are very important. In this study, the computational domain is chosen as 35D in flow and 20D in vertical direction, and the first cylinder was situated at 8D distance away from the inlet.

RESULTS AND DISCUSSIONS

Configuration of the square cylinders in the flow field is shown in Figure 1. Flow regimes around cylinders are classified according to vortex formation between the cylinders and the interaction of these vortices with the shear layer of the downstream cylinder.

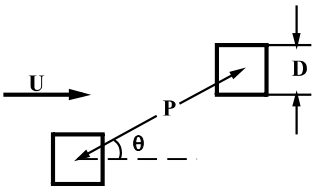

Figure 1 Arrangement the square of the cylinders

Flow regimes

Flow regimes are classified according two interaction of the shear layer separated from upstream cylinder and downstream cylinder as; single vortex suppression and single vortex street, vortex impingement, shear layer reattachment, induced separation, bistable gap flow and, synchronized vortex formation.

Vortex suppression and single vortex street

Even though, there is a vortex street behind a cylinder in a free stream flow at the Reynolds numbers larger than the value of 50, the existence of the second cylinder close the first one suppress the formation of vortex street at the downstream region at relatively small Reynolds numbers (Figure 2 (a)). As the Reynolds number increases, the boundary layer separation from the first cylinder forms a vortex street behind the wake region of the downstream cylinder (Figure 2 (b)). In both cases, the fluid between the two cylinders is stationary.

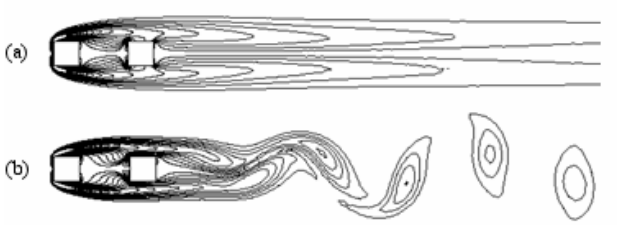

Figure 2 Flow between the cylinders and in the wake region for P/D= 3, θ = 0 in case of (a) Re=100, (b) Re=200

Vortex impingement

As the distance between the cylinder increases beyond the critical spacing at the small incidence angles, the shear layer separated from upper and lower side of the upstream cylinder form vortices between the cylinders (Figure 3). These vortices impinge upon the downstream cylinder and then, by joining the shear layer separated from downstream cylinder, form vortex street at the downstream region.

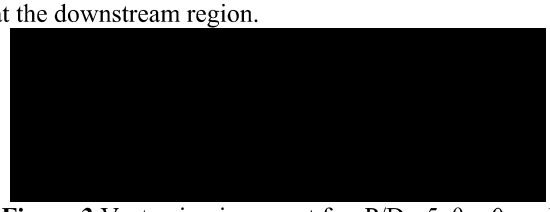

Figure 3 Vortex impingement for P/D= 5, θ = 0 and Re=200

Shear layer reattachment

At the small spacing between the cylinders and small incidence angles, shear layer reattachment on the downstream cylinder is observed. Separated boundary layer from upper site of the upstream cylinder contacts the downstream cylinder, and combining with the separated shear layer from the downstream cylinder to form a vortex street behind it. As seen in Figure 4, for Re=200, the vortex formations are closer to the cylinder comparison that for Re = 100..

Figure 4 for P/D=2 and θ = 15, Shear layer reattachment flow (a) Re=100, (b) Re=200

Induced separation

Relatively larger cylinder spacing and incidence angles, induced separation type flow observed (Figure 5). At this flow type, a gap flow between the cylinders occurs and this flow prevents the vorticity generation from inner surface of the upstream cylinder. The separated shear layer from inner and outer surface of the upstream cylinder join the vortex formed from downstream cylinder.

Figure 5 For P/D=3, θ=30, Induced separation flow (a) Re=100, (b) Re=200

Bistable gap flow

At the small cylinder spacing and large incidence angles, fluid flow switces between the cylinders at the bistable manner towards to wake of upstream cylinder and downstream cylinder (Figure 6). Figure 6 (a) presents flow between the gap towards to wake of top cylinder and causes narrow and broad wake at the up cylinder and down cylinders respectively. At figure 6 (b) gap flow direction is approximately along the centerline and wakes behind the cylinders are approximately at the same size. Figure 6(d), the flow is directed towards the wake region of the bottom cylinder.

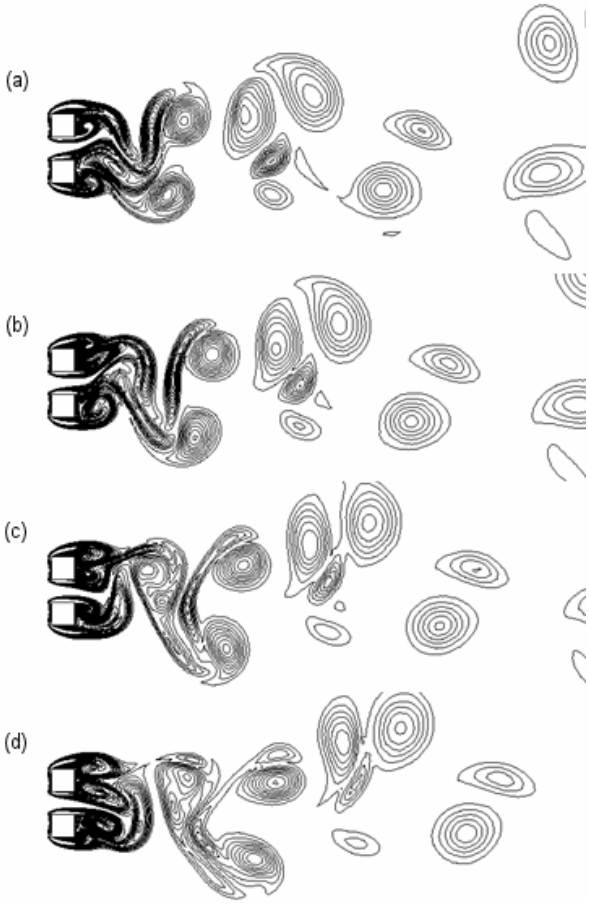

Figure 6 Bistable gap flow between the cylinders (P/D=2, Re=200, θ=90)

Synchronized Vortex Formation

At the large spacing and incidence angles of 70, 75 and 90º synchronized vortex formations are observed in the downstream region (Figure 7). These vortex formations would be in phase, anti phase or complex forms depending on incidence angle.

In Figure 7(a), complex type vortex interaction appears at the wake of both cylinders at the high incidence angles. Vorticies are formed further downstream of the upstream cylinder than that of downstream one. As the incidence angle increases (figure 7 (b)), the boundary layer separations take place from the same side surfaces and the vortex streets are formed almost at the same distance to the cylinders. For θ = 90, (Figure 7(c)), the vorticies formed from opposite surface of the cylinders and vortex streets are symmetrical.

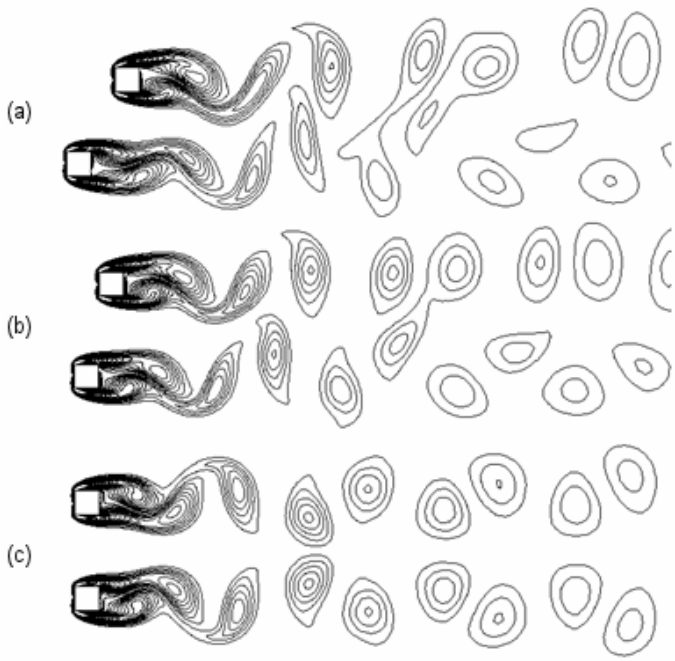

Figure 7 Synchronized vortex formation (P/D=4, Re=100) (a) θ=70, (b) θ=75, (c) θ=90

FORCES ACTING ON CYLINDERS

The variation of the mean drag coefficient and square root mean of the lift coefficient has been reported at different pitch ratios and incidence angles.

The Drag Coefficient

In Figure 8, for Re=200, the drag coefficients of both cylinders are depicted as a function of the distance between the cylinder centers (P/D) and the incidence angle (θ). For P/D=2 and 3 of θ = 0, the mean drag coefficient of the downstream cylinder takes negative values since no vortex formation is observed between the cylinders. As the incidence angle is increased, with the boundary layer separation from the upstream cylinder, the drag coefficient of the downstream cylinder increases. For θ > 30, except for P/D=2, the lift coefficient of both cylinders approach the same value. The largest lift coefficient is observed in P/D=2 and θ =75 case where the flow between the two cylinders is bistable.

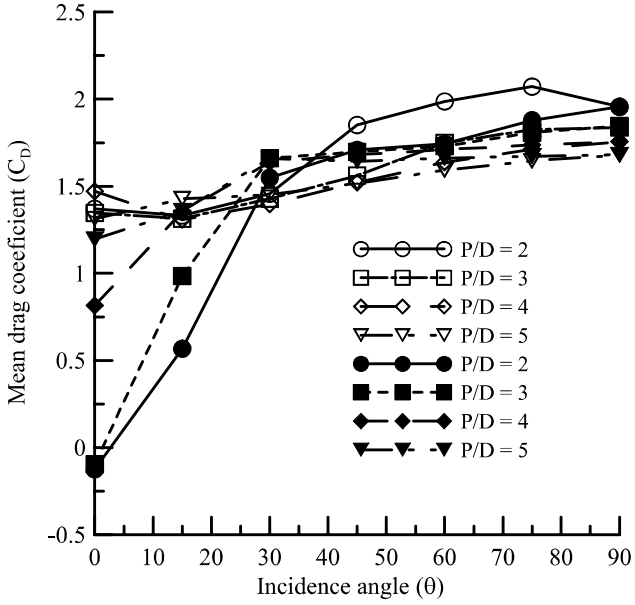

Figure 8 The variation of the drag coefficient with P/D and the incidence angle for Re=200. Filled symbols indicate the downstream cylinder

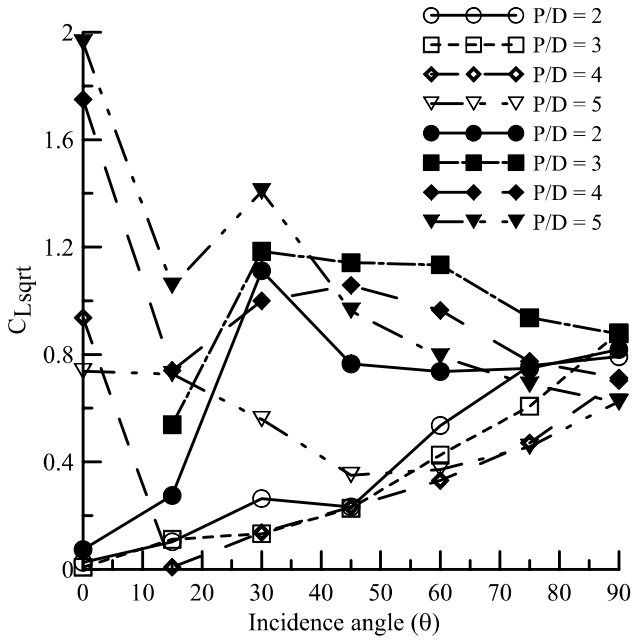

Figure 9 Variation of the root mean square root values of lift coefficient with P/D and the incidence angle for Re=200. Filled symbols indicate the downstream cylinder

The Lift Coefficient

The root mean square root values of lift coefficients on both cylinders are shown in Figure 9 in terms of the distance between the cylinder centers (P/D) and the incidence angle (θ). The lift coefficient takes the maximum values for P/D=4 and 5 of θ =0 on the downstream cylinder where the occurring

vortices between the cylinders impinge on the downstream cylinder.

As the incidence angle is increased (θ = 15), vortex formation between the cylinders turns to shear layer reattachment flow and the value of C_{Lsqrt} of downstream cylinder decreases. For θ = 30, vortex formation from both cylinders occur and the value of C_{Lsqrt} of downstream cylinder increases. As the incidence angle is further increased, the value of C_{Lsqrt} of downstream cylinder decreases. When the incidence angle approaches to 90, the difference between C_{Lsqrt} values of both cylinders closes.

THE STROUHAL NUMBER

In Figure 10, the power spectrum of the Strouhal numbers are depicted for various flow patterns. Left and right columns present spectrums taken from lift coefficients on the upstream and downstream cylinder respectively. Figure 10 (a) and (b) reports the power spectrums for the case of vortex impinging flow (Figure 3). This flow characterized by slender peaks for the vortex formation frequency and its harmonics. Vortex impinging on the downstream cylinder causes the larger amplitude responses on the downstream cylinder than that on upstream one.

Figure 10 (c) and (d) reports the power spectrum of Shear layer reattachment flow (figure 4) for Reynolds number of 200. In this flow case, slender peaks appear at the vortex shedding frequency and its first harmonic similar to vortex impinging flow but with smaller amplitudes.

In case of the induced separation flow (figure 5), complex interactions of the vortices at the downstream region produces broader peaks at the lower frequencies (figure 10 (e), (f)) in comparison to aforementioned flow cases.

In case of the bistable gap flow, the non-periodic flow between the cylinders (figure 6) produces broad and approximately at the same amplitude peaks on the upstream and downstream cylinders (figure 10 (g) and (h)).

In the synchronized vortex formation flow (figure 7), again slender peaks appear only at the vortex shedding frequencies (figure 10 (j), (k)).

CONCLUSION

In this study, the flow patterns and the corresponding forces on the downstream and upstream cylinders have been studied for staggered configuration of two square cylinders at the Reynolds numbers of 100 and 200. The laminar flow pass the staggered cylinders exhibits some of the flow structures such as single vortex street, vortex impingement, shear layer reattachment, induced separation, bistable flow and synchronized vortex formation that previously observed in the wake of circular cylinders and high Reynolds numbers

In addition to flow structures, variation of the mean drag coefficient and square root of the lift coefficient also obtained for different pitch ratios and incidence angles. For P/D = 2, 3 and θ = 0, mean values of the drag coefficient on the downstream cylinder takes negative values. At the bistable flow, switching of the gap flow between the cylinder leads to broader peak response at the power spectrum.

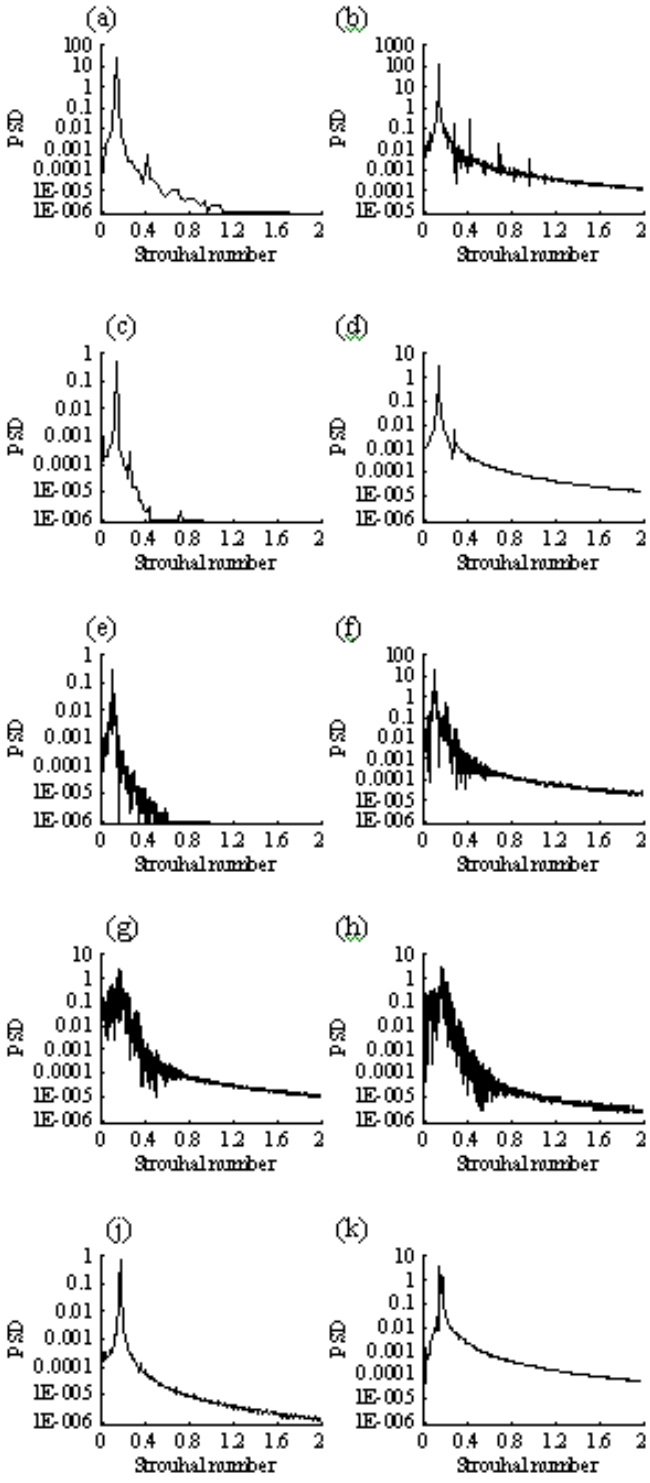

Figure 10 Variation of the power spectrums on the upstream ((a), (c), (e), (g), (j)) and downstream cylinders ((b), (d), (f), (h), (k)) with flow patterns. Vortex impinging (a) and (b), shear layer reattachment (c) and (d), induced separation (e) and (f), bistable (g) and (h), synchronized vortex formation (j) and (k).

REFERENCES

[1] Zdravkovich, M. M., 1985, Flow induced oscillation ot two interfering circular cylinders, *Journal of Sound and Vibration*, Vol. 101, 1985, pp. 511-521.

[2] Sumner, D., Price, S. J. and Paidoussis, M. P., Flow-pattern identification for two staggered circular cylinders in cross-flow, *Journal of Fluid Mechanics*, Vol. 411, 2000, pp. 273-303.

[3] Sumner, D., Richards, M. D., Akosile, O.O., Two staggered circular cylinders of equal diameter in cross-flow, *Journal of Fluids and Structures* Vol. 20, 2005, pp. 255-277.

[4] Price, S. J, and Paidoussis, M. P., The aerodynamic forces acting on groups of two and three circular cylinders when subjected to a cross-flow, *Journal of Wind Engineering and Industrial Aerodynamics*, Vol. 14, 1984, pp. 329-347.

[5] Gu, Z., Sun, T., On interference between two circular cylinders in staggered arrangement at high subcritical Reynolds number, *Journal of Wind and Industrial Aerodynamics,* Vol. 80, 1999, pp. 287-309.

[6] Mittal, S., Kumar, V., Raghuvanshi, A., Unsteady incompressible flows past two cylinders in tandem and staggered arrangements, *International Journal for NumericalMmethods inFfluids*, Vol. 25, 1997, pp. 1315-1344.

[7] Carmo B. S., Sherwin S. J., Bearman P. W., and Willden R. H. J., Wake transition in the flow around two circular cylinders in staggered arrangements, *Journal of Fluid Mechanics*, Vol. 597, 2008, pp. 1-29.

[8] Jester, W. and Kallinderis, Y., Numerical study of incompressible flow about fixed cylinder pairs, *Journal of Fluid and Structures*, Vol. 17, 2003, pp. 561-577.

[9] Fluent, 2003 FLUENT, Inc., FLUENT 7.1 User's Guide, 2003, Lebanon: NH.

[10] Mahir N and Altaç Z, Numerical investigation of convective heat transfer in unsteady flow past two cylinders in tandem arrangements, *International Journal of Heat and Fluid Flow*, Vol. 29, 2008, pp. 1309–1318.